ACS Medicinal Chemistry Letters

Letter

pubs.acs.org/acsmedchemlett

1,3-Dimethyl Benzimidazolones Are Potent, Selective Inhibitors of the BRPF1 Bromodomain

Emmanuel H. Demont,[†] Paul Bamborough,[*,‡] Chun-wa Chung,[‡] Peter D. Craggs,[‡] David Fallon,[†] Laurie J. Gordon,[‡] Paola Grandi,[§] Clare I. Hobbs,[‡] Jameed Hussain,[‡] Emma J. Jones,[‡] Armelle Le Gall,[‡] Anne-Marie Michon,[§] Darren J. Mitchell,[†] Rab K. Prinjha,[†] Andy D. Roberts,[∥] Robert J. Sheppard,[†] and Robert J. Watson[†]

[†]Epinova Discovery Performance Unit and [‡]Molecular Discovery Research, GlaxoSmithKline, Gunnels Wood Road, Stevenage, Hertfordshire SG1 2NY, U.K.

[§]Cellzome GmbH, Molecular Discovery Research, GlaxoSmithKline, Meyerhofstrasse 1, 69117 Heidelberg, Germany

[∥]DMPK, GlaxoSmithKline, Park Road, Ware SG12 0DP, U.K.

Supporting Information

ABSTRACT: The BRPF (bromodomain and PHD finger-containing) protein family are important scaffolding proteins for assembly of MYST histone acetyltransferase complexes. Here, we report the discovery, binding mode, and structure−activity relationship (SAR) of the first potent, selective series of inhibitors of the BRPF1 bromodomain.

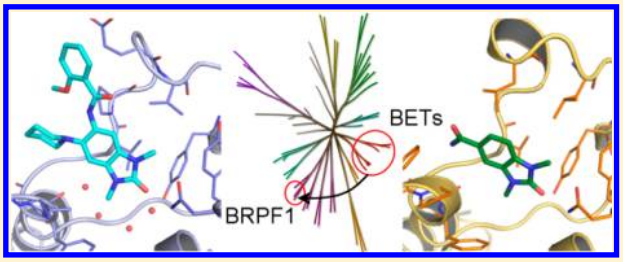

KEYWORDS: *BRPF1, BRPF2, BRD1, BRPF3, bromodomain, chemical probe, epigenetics, fragment, inhibitor*

Bromodomain modules are found within a diverse group of chromatin-regulator proteins and act as specific readers of acetylated lysine (KAc) residues. The BET (bromodomain and extra terminal) subfamily (BRD2/3/4/T) has received much attention following the discovery that inhibitors found using cellular screens bind to these targets and act by blocking their binding to Nε-acetyl-lysine (KAc) modified histones.[1−3] BET inhibitors such as I-BET762 and RVX-208 have progressed into the clinic for oncology and cardiovascular disease,[1,4] and their use as chemical probes has enabled extensive biology of the BET proteins to be elucidated.[5]

The functions of other bromodomain-containing proteins (BCPs) are less well understood. The availability of small-molecule probes for these would signficantly enhance our ability to dissect their biological roles and therapeutic relevance. While some disease rationale exists for a few BCPs,[6] their multidomain architecture and location within multiprotein complexes makes it difficult to attribute observed functions specifically to the bromodomain. The BRPF (bromodomain and PHD finger-containing) family, BRPF1, BRPF2/BRD1, and BRPF3, which operate as scaffolds to assemble complexes of MYST-family histone acetyltransferases (HATs), are excellent examples of this (Figure S1, Supporting Information).[7]

BRPF1, a component of complexes containing the MOZ/MORF transcriptional coactivators, links the catalytic HATs to the other subunits ING5 and hEAF6.[8] Translocations of MOZ are associated with aggressive subtypes of leukemia, producing, for example, the MOZ-TIF2 fusion protein, which also interacts with BRPF1.[8] BRPF1 is important for maintaining Hox gene expression and skeletal development in fish.[9] BRPF2 (BRD1) preferentially forms complexes with ING4 and another MYST family HAT, HBO1. HBO1 acetylates H3K14 and promotes erythroid differentiation.[10] BRPF2 has been linked to bipolar disorder and schizophrenia in European populations.[11]

Some functions of the BRPFs have been mapped to individual domains. The histone-binding modules include a PZP (PHD-Zn knuckle-PHD) domain, which in BRPF1 and BRPF2 binds unmodified histone H3K4.[12] The C-terminal PWWP domain of BRPF1 binds H3K36me3 and localizes BRPF1 to condensed chromatin of mitotic cells.[9,13] Like other bromodomains, that of BRPF1 binds KAc peptides, including H2AK5ac, H3K14ac, and H4K12ac.[9,14] Despite these important observations, the therapeutic opportunities of targeting the bromodomain remain unclear. For example, deletion of the BRPF1 bromodomain does not prevent the acetylation of histone H3 by the HBO1/BRPF1 complex.[15] We report here the discovery of selective, potent BRPF1 bromodomain inhibitors, which will help to unravel the functions of this complex protein.

The BRPF bromodomains themselves are highly conserved, sharing >65% sequence identity over their ∼100 amino acids

Received: July 22, 2014
Accepted: August 28, 2014

   dx.doi.org/10.1021/ml5002932 | *ACS Med. Chem. Lett.* XXXX, XXX, XXX−XXX

(Figure S1, Supporting Information). Their KAc sites closely resemble other bromodomains, including those of the BETs, for which small-molecule inhibitors have been discovered via a wide range of approaches.[16,17]

The common features of the KAc binding sites of BET and CREBBP, for example, bind fragments such as acetaminophen in a similar manner.[18] In addition, BET KAc site fragments have been optimized for potency and selectivity by targeting nearby regions of the site.[19−21] It seemed likely that other bromodomains would be tractable to this approach, so we set out to generate selective inhibitors of the BRPFs following the strategy of optimizing the selectivity of an initially nonselective KAc site fragment.

One important factor to consider is that inhibition of the BET bromodomains leads to significant and diverse phenotypic responses.[5] It is critical therefore that a BRPF1 probe molecule has a high degree of selectivity over the BET proteins to ensure that biological insights can be confidently ascribed to BRPF1 and not to BET. We consider that a minimum selectivity window of 2 logs over BET is needed, preferably 3 logs if possible.

The BRPF1 starting fragment **1** (Figure 1a) was initially found in a nuclear magnetic resonance screen (STD-NMR,

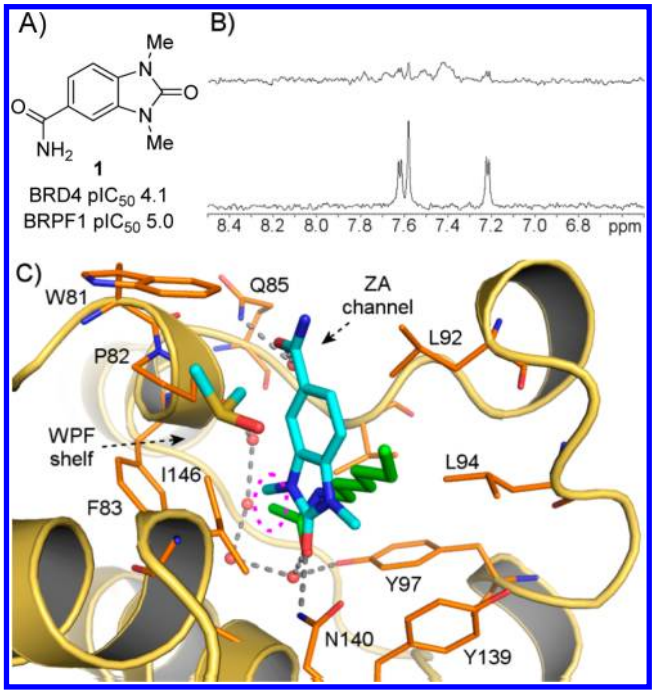

Figure 1. (A) Fragment **1**. (B) Lower: STD spectrum of fragment **1** with 5 μM BRD4(1−477). Upper: same, in the presence of 1 mM competitive ligand GW841819. (C) X-ray structure of **1** (cyan) bound in the KAc site of BRD4 (with a DMSO molecule on the WPF shelf). An acetylated lysine side chain from a histone peptide BRD4 complex is superimposed (green, PDB code 3uvw).[22] Hydrogen bonds are indicated with dashed gray lines. The acetyl methyl pocket is ringed by a broken magenta line.

Supplementary Methods, Supporting Information) against the N-terminal bromodomain of BRD4 (BRD4-BD1). The STD signal was effectively competed by the addition of GW841819, a BRD4 KAc site binding inhibitor (Figure 1b).[2] The pIC_{50} of fragment **1** for BRD4-BD1 was determined to be 4.1 by TR-FRET competition binding.

A crystal structure of BRD4 BD1 in complex with **1** was solved. The carbonyl oxygen of the benzimidazolone makes interactions mimicking those of the KAc side chain (Figure 1c). Both form the same two hydrogen-bonds, with the side chain NH_2 of Asn140, and via a through-water interaction to the OH of Tyr97. The N1-methyl group occupies the terminal methyl pocket of the acetyl recognition site near Phe83. These interactions are typical of most BET inhibitors described to date.[16,18] The primary carboxamide of **1** makes no direct interactions with the protein but does H-bond indirectly to Gln85 through a water molecule.

The residues directly interacting with fragment **1** and the conserved waters define a recognition motif for the KAc headgroup common to typical bromodomains (Figure S1, Supporting Information). Fragments that bind to this site can potentially act as scaffolds for inhibitors of multiple bromodomains, with potency and selectivity governed by substituents, which project into less conserved parts of the site, as is the case for the BETs.[19−21] One significant difference between BRD4 and BRPF1 is the "gatekeeper" residue that forms one wall of the KAc site.[2] In BET family BD1 bromodomains this is isoleucine (Ile146 in BRD4, Figure 1c), and in BD2, it is valine. In the BRPF family this is a larger phenyalanine residue, which restricts the space accessible to inhibitors (Figure S1b, Supporting Information).

As part of our inhibitor discovery strategy, we assembled a set of molecules targeting the bromodomain KAc site. These included analogues derived from BET-binding fragments such as **1**, obtained by searching our compound collection and purchased libraries. When this set was screened against the BRPF1 bromodomain, the hits included a cluster of molecules containing the 1,3-dimethyl benzimidazolone moiety. The hits were also tested against BRD4 BD1. Figure 2 shows the results

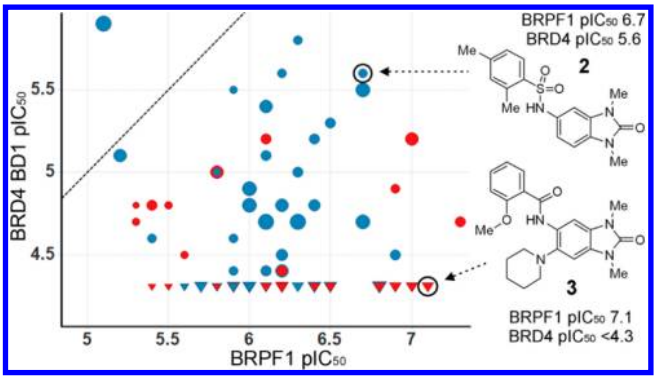

Figure 2. Selectivity of initial 1,3-dimethyl benzimidazolones for BRPF1 over BRD4 BD1, with the line of unity (dashed). Red = 5-amides; blue = 5-sulfonamides. The size of the points is proportional to molecular weight. Circles indicate fitted BRD4 BD1 curves, and triangles indicate BRD4 BD1. pIC_{50} <4.3. Example hits **2** and **3** are marked.

for benzimidazolones from the focused set. Among the most active hits were sulfonamides such as **2** and amides such as **3**. We chose to concentrate on the (5,6)-disubstituted benzimidazolones, in particular amides related to **3**, because of the large window of selectivity of this compound for BRPF1 over BRD4.

Hits were tested in a $^{15}N-^{1}H$ HSQC NMR assay (Supplementary Methods, Supporting Information) to verify direct binding to the BRPF1 bromodomain. Compounds **1**, **2**, and **3** caused strong and specific shifts (Figure S2, Supporting

dx.doi.org/10.1021/ml5002932 | ACS Med. Chem. Lett. XXXX, XXX, XXX−XXX

Information). Consistent with the expected binding mode, residues close to the KAc binding site were perturbed, e.g., Ile652 and Phe653, which line one side of the pocket (Figure 3). Other residues are not perturbed, for example, Leu688, which lies >20 Å distant from the site.

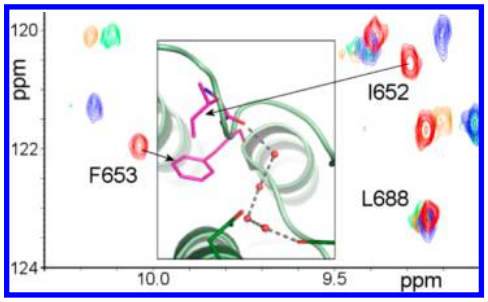

Figure 3. $^{15}N-^{1}H$ HSQC chemical shift of residues Ile652 and Phe653 of the BRPF1 bromodomain (red), which move on the addition of 1 mM **1** (blue), **2** (green), or **3** (orange). Inset: location of Ile652 and Phe653 (magenta) within the KAc site.

We reasoned that the binding mode of the dimethyl benzimidazolone core in BRPF1 would mimic that of fragment **1** in BRD4. Because the core is symmetrical, it was unclear which of the N1 or N3 methyl groups of **3** would occupy the conserved acetyl methyl pocket of BRPF1. Molecular modeling suggested that this might be very substituent-dependent. To answer that question, analogues **4** and **5**, in which each of the two *N*-methyl groups were removed in turn, were prepared according to Scheme 1. Fluorinated mono- or di-*N*-alkylated

Scheme 1. Synthesis of Compounds 3, 4, and 5[a]

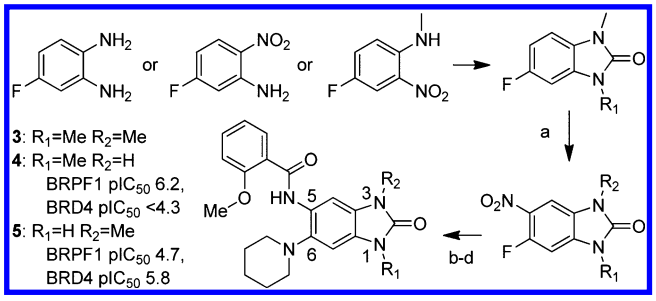

[a]Reagents and conditions: (a) fuming HNO_3, $(CH_3CO)_2O$, −30 to 0 °C, 71−81%; (b) piperidine, DIPEA, DMSO, 120 °C, microwaves, 52−79%; (c) H_2, Pd/C, EtOH, room temperature, 66−99%, or Fe(0), NH_4Cl, EtOH, 90 °C, 21%; (d) 2-MeO-PhCOCl, pyridine, CH_2Cl_2 or DMF, room temperature, 30−55%.

benzimidazolones can be nitrated in a regioselective manner.[23] Displacement of the fluorine via SNAr by piperidine followed by reduction of the nitro group and amide formation led to the required analogues in good yields (Synthetic Methods, Supporting Information).

It was expected that the methyl group occupying the acetyl methyl pocket would be the more important group for binding. Relative to the dimethyl parent **3**, both des-methyl compounds **4** and **5** lost BRPF1 potency (Scheme 1). However, the N1−H compound **5** lost 2.4 logs of activity with respect to **3**, while the N3−H isomer **4** lost only 0.9. We concluded that **3** probably binds to BRPF1 with its N1-methyl buried in the acetyl methyl pocket close to Phe653 and to BRD4 in an analogous way.

Very shortly afterward, a 1.65 Å resolution crystal structure of the BRPF1 bromodomain in complex with **3** was obtained. The whole molecule can clearly be seen in the electron density, and the binding mode is similar in both chains of the asymmetric unit (Figure S3, Supporting Information). The structure shows that the benzimidazolone core of **3** binds to BRPF1 in a very similar way as does fragment **1** to BRD4 (Figure 4a). The N1-methyl group does indeed bind in the

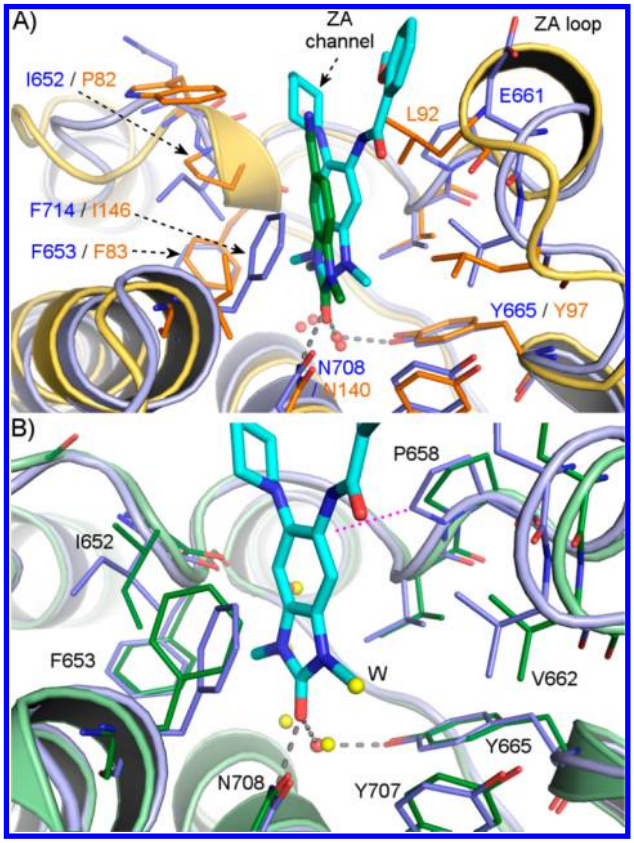

Figure 4. (A) X-ray structure of BRPF1/compound **3** (blue) and of BRD4 BD1 (orange)/fragment **1** (green). (B) The complex of BRPF1 with **3** (blue) compared to apo BRPF1 (green, PDB code 4lc2). Water molecules in the apo structure are shown in yellow; the water displaced by the N3-methyl group is labeled as W.

acetyl methyl pocket of BRPF1 near Phe653, while the C2-carbonyl interacts with the conserved asparagine Asn708 and via water to Tyr665 (in the same way as that of **1** with the equivalent BRD4 residues Asn140 and Tyr97). The replacement of the Ile146 gatekeeper residue in BRD4 with the bulky Phe714 in BRPF1 results in a tilt in binding mode of the benzimidazolone core between the two bromodomains.

The decrease in BRPF1 potency of 0.9 logs upon removal of the N3-methyl (compare **4** to **3**) can be rationalized by comparing the BRPF1 complex with **3** to the literature apo X-ray structure (Figure 4b). The N3-methyl of **3** binds in a relatively lipophilic environment, close to the side chains of Tyr707 and Val662. A water molecule is found there in the apo structure, so its displacement by the N3 methyl group may allow for favorable hydrophobic interactions with these residues. In support of this interpretation, upon binding of **3** the side chain of Val662 moves toward the N3 methyl group by about 1 Å (Figure 4b).

dx.doi.org/10.1021/ml5002932 | ACS Med. Chem. Lett. XXXX, XXX, XXX−XXX

The X-ray structure can also help to rationalize the structure−activity relationship (SAR) of close analogues of **3**. Table 1 summarizes variation at the benzimidazolone 5-

Table 1. pIC_{50} at the Benzimidazolone 5-Position[a]

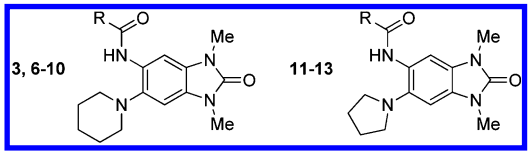

R	no.	BRPF1	BRD4 BD1	no.	BRPF1	BRD4 BD1
2-methoxy phenyl	**3**	7.1	<4.3	**11**	7.3	≤4.7
3-methoxy phenyl	**6**	7.0	<4.3	**12**	6.5	<4.3
phenyl	**7**	7.0	<4.3			
2-methyl phenyl	**8**	6.5	<4.3			
t-butyl	**9**	6.2	<4.3			
benzyl	**10**	6.4	<4.3	**13**	6.1	<4.3

[a]See also Table S1, Supporting Information.

position amide substituent, when the 6-piperidine substituent is retained (compounds **6**−**10**). Where close analogues with pyrrolidine at the 6-position were available, these were also tested (Table 1, compounds **11**−**13**).

The 5-position amide substituent of **3** interacts with residues of the BRPF1 ZA loop (Figure 4a). The 2-methoxy phenyl **3** is marginally more potent than the 3-methoxy phenyl carboxamide **6** and unsubstituted phenyl **7**. This trend is more pronounced with other analogues tested (including the directly analogous pyrrolidine pair, **11** and **12**, and others shown below). Any preference for the 2-methoxy phenyl substituent is not solely a steric effect because the 2-methyl phenyl **8** is weaker than **7**. In its bound conformation, the methoxy group forms an internal hydrogen-bond to the NH group of the carboxamide linker, resulting in a relatively rigid planar structure (Figure 4a). This presumably assists packing of the face of the phenyl ring with the side chain methylene groups of Glu661 (Figure 5). Aliphatic analogues such as the *t*-butyl carboxamide **9** and the benzyl carboxamides **10** and **13**, which would be unable to pack against this side chain so efficiently, are significantly less potent (Table 1).

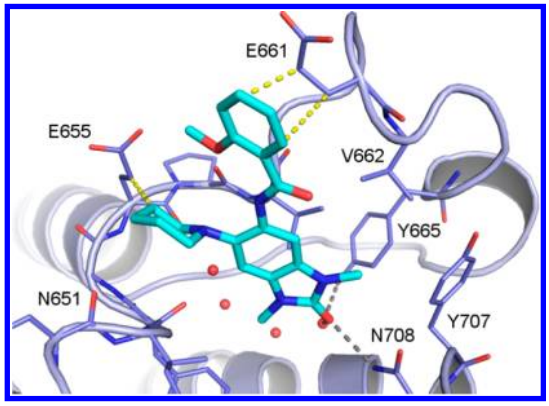

Figure 5. X-ray structure of BRPF1 with **3**, showing lipophilic interactions between the 5- and 6-substituents and the protein (E655 and E661) as yellow dotted lines.

Table 2 shows compounds modified at the 6-position in the 5-(2-methoxyphenyl) carboxamide series. Data for 3-methoxy

Table 2. pIC_{50} at the Benzimidazolone 6-Position[a]

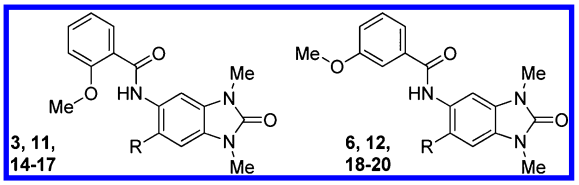

R	no.	BRPF1	BRD4 BD1	no.	BRPF1	BRD4 BD1
1-piperidine	**3**	7.1	<4.3	**6**	7.0	<4.3
1-pyrrolidine	**11**	7.3	≤4.7	**12**	6.5	<4.3
4-morpholine	**14**	6.9	<4.3	**18**	6.2	<4.3
methoxy	**15**	6.9	≤4.9			
methyl	**16**	5.8	<4.3	**19**	5.5	<4.3
H	**17**	5.6	<4.3	**20**	5.5	4.8

[a]See also Table S1, Supporting Information.

analogues are also shown for comparison. The trends are similar, although as outlined above the 2-methoxy compounds are always more potent than their 3-methoxy analogues.

The 6-piperidine substituent of **3** makes few close contacts with the bromodomain apart from a small hydrophobic patch on the side chain methylene of Glu655 (Figure 5). The size of the ring makes little consistent difference to BRPF1 potency (compare **11** to **3**, and **12** to **6**). Interestingly, the morpholines **14** and **18** are slightly weaker than the corresponding piperidines **3** and **6**. This is probably due to the proximity of the backbone carbonyl of Asn651 to the 4-position of the piperidine ring (3.5 Å, Figure 5), which would disfavor electronegativity in this region.

Smaller 6-substituents, such as the methoxy **15**, are tolerated by BRPF1 with relatively little loss of activity, although the methyl and hydrogen analogues **16**, **17**, **19**, and **20** are weaker. Rather than being due to the size of the substituents, this may reflect the loss of an oxygen or nitrogen atom at the substituent point itself. The piperidine N1 electrostatically favors the bound conformation of the amide at the 5-position (Figure 5) over the alternative where the amide carbonyl points toward the piperidine.

Examination of the data suggests that in general compounds with smaller 6-substituents (e.g., **15** and **17**) have BRD4 pIC_{50}s closer to the measurable threshold of 4.3 than larger ones such as **3** and **14** (Tables 2 and S1, Supporting Information). There is a trend toward greater selectivity for BRPF1 over BRD4 with increasing size of this substituent. In BRD4, this vector would point toward the narrow ZA channel between Trp81 and Leu92 (Figure 4a), perhaps explaining this result.

All compounds are selective for BRPF1 over BRPF2/3, an unexpected finding given the conservation between their KAc sites. Subtle differences close to the KAc pocket must contribute to this because even fragment **1** shows this trend (Table S1, Supporting Information). We speculate that the substitution of Ser592 in BRPF2 or Asn619 in BRPF3 for Pro658 in BRPF1 may contribute. The benzimidazolone C5 atom of **3** and the Pro658 Cδ carbon of BRPF1 are close enough for a hydrophobic contact (Figure 4b, 3.8 Å). No X-ray structure of BRPF3 has been solved, but in BRPF2 the backbone NH of Ser592 H-bonds to a water molecule in chain A. Superimposing BRPF1 and BRPF2 suggests that the aromatic benzimidazolone ring might be unfavorably close to,

dx.doi.org/10.1021/ml5002932 | ACS Med. Chem. Lett. XXXX, XXX, XXX−XXX

or displace, this water in BRPF2 (Figure S5, Supporting Information).

Compound **3** was tested in the BROMO*scan* panel of 35 bromodomain binding assays. Consistent with the data above, it showed excellent BRPF1 potency (pK_d = 8.0) and a good window of selectivity over the BETs and BRPF2/3. In addition, it was highly selective over other bromodomains tested (Table S2, Supporting Information).

A cellular protein interaction assay measuring the displacement of NanoLuc-tagged BRPF1 bromodomain from Halo-tagged histone H3.3 was employed to demonstrate cell permeability and disruption of chromatin binding (Supplementary Methods, Supporting Information).[24] Compound **3** exhibited a dose−response curve with micromolar IC_{50}, while the less active analogue **5** showed no effect (Figure 6b). When

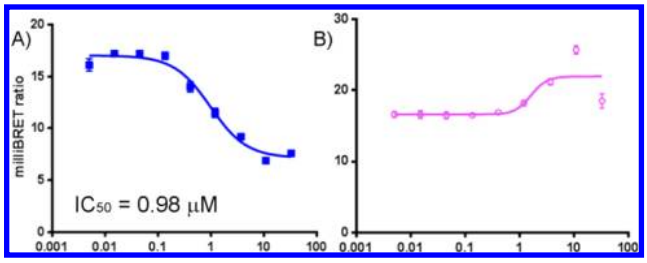

Figure 6. BRPF1 isoform 1 bromodomain NanoBRET dose−response curves of (A) compound **3** and (B) analogue **5**.

BRPF1 isoform 2 (containing an insertion in the bromodomain at Ser660) was used instead, neither compound showed any effect, consistent with a KAc site competitive mode of action (Figure S6, Supporting Information).

To conclude, in compound **3** we have discovered a potent inhibitor of the BRPF1 bromodomain whose properties are summarized in Table 3. It has excellent selectivity over other bromodomains, is cell permeable, and displaces the BRPF1 bromodomain from Histone H3.3. Future publications will describe the optimization of this series.

Table 3. Summary of Properties of Compound 3

BRPF1/2/3 pIC_{50} (TR-FRET)	7.1/5.1/<4.0
BRD4 BD1/BD2 pIC_{50} (TR-FRET)	<4.3/<4.3
BRPF1 NanoBRET pIC_{50}[a]	6.0
BROMO*scan* selectivity over other bromodomains[b]	BETs, ∼3 logs BRPF2/3, ∼2 logs all others, >2 logs
aqueous solubility (CLND)	low (25 μM)
artificial membrane permeability	high (3.5×10^{-5} cm/s)

[a]Promega Corp. (Figure S6, Supporting Information). [b]DiscoveRx Corp. (Table S2, Supporting Information).

■ ASSOCIATED CONTENT

Supporting Information

Synthetic procedures, analytical data, methods, and figures. This material is available free of charge via the Internet at http://pubs.acs.org.

Accession Codes

X-ray structures have been deposited in the PDB with accession codes 4uyd and 4uye. Compound **3** is available from Chemdiv (cat. # C301-5895) and Princeton Biomolecular Research (cat. # OSSK_ 842278).

■ AUTHOR INFORMATION

Corresponding Author

*(P.B.) E-mail: paul.a.bamborough@gsk.com. Tel: +44 1438 763246. Fax: +44 1438 763352.

Notes

The authors declare no competing financial interest.

■ ACKNOWLEDGMENTS

We thank Jacqui Méndez and Danette Daniels of Promega Corporation for facilitating NanoBRET assays, and the DiscoveRx Corp. for BROMO*scan* screening. Thanks to Heather Barnett, Mark Bird, and Tony Cooper for chemistry and discussion, Paul Homes for fermentation, Oxana Polyakova for BRD4 protein preparation, Richard Upton for NMR support, Abigail Lucas, Phylicia Dassardo-Joseph, and Helena Yong for crystallization assistance, and Melanie Leveridge for help during manuscript preparation.

■ ABBREVIATIONS

BD1, bromodomain; BET, bromodomain and extra-terminal; BRD1−4, bromodomain containing 1−4; BRPF, bromodomain and PHD finger-containing; KAc, acetyl-lysine; PWWP, Pro-Trp-Trp-Pro

■ REFERENCES

(1) Nicodeme, E.; Jeffrey, K. L.; Schaefer, U.; Beinke, S.; Dewell, S.; Chung, C. W.; Chandwani, R.; Marazzi, I.; Wilson, P.; Coste, H.; White, J.; Kirilovsky, J.; Rice, C. M.; Lora, J. M.; Prinjha, R. K.; Lee, K.; Tarakhovsky, A. Suppression of inflammation by a synthetic histone mimic. *Nature* **2010**, *468*, 1119−1123.

(2) Chung, C.; Coste, H.; White, J. H.; Mirguet, O.; Wilde, J.; Gosmini, R. L.; Delves, C.; Magny, S. M.; Woodward, R.; Hughes, S. A.; Boursier, E. V.; Flynn, H.; Bouillot, A. M.; Bamborough, P.; Brusq, J. M.; Gellibert, F. J.; Jones, E. J.; Riou, A. M.; Homes, P.; Martin, S. L.; Uings, I. J.; Toum, J.; Clement, C. A.; Boullay, A. B.; Grimley, R. L.; Blandel, F. M.; Prinjha, R. K.; Lee, K.; Kirilovsky, J.; Nicodeme, E. Discovery and characterization of small molecule inhibitors of the BET family bromodomains. *J. Med. Chem.* **2011**, *54*, 3827−3838.

(3) Filippakopoulos, P.; Qi, J.; Picaud, S.; Shen, Y.; Smith, W. B.; Fedorov, O.; Morse, E. M.; Keates, T.; Hickman, T. T.; Felletar, I.; Philpott, M.; Munro, S.; McKeown, M. R.; Wang, Y.; Christie, A. L.; West, N.; Cameron, M. J.; Schwartz, B.; Heightman, T. D.; La, T. N.; French, C. A.; Wiest, O.; Kung, A. L.; Knapp, S.; Bradner, J. E. Selective inhibition of BET bromodomains. *Nature* **2010**, *468*, 1067−1073.

(4) McLure, K. G.; Gesner, E. M.; Tsujikawa, L.; Kharenko, O. A.; Attwell, S.; Campeau, E.; Wasiak, S.; Stein, A.; White, A.; Fontano, E.; Suto, R. K.; Wong, N. C.; Wagner, G. S.; Hansen, H. C.; Young, P. R. RVX-208, an inducer of ApoA-I in humans, is a BET bromodomain antagonist. *PLoS One* **2013**, *8*, e83190.

(5) Muller, S.; Knapp, S. Discovery of BET bromodomain inhibitors and their role in target validation. *MedChemComm* **2014**, *5*, 228−296.

(6) Chung, C.; Tough, D. Bromodomains: a new target class for small molecule drug discovery. *Drug Discovery Today: Ther. Strategies* **2012**, *9*, e111−e120.

(7) Carlson, S.; Glass, K. C. The MOZ histone acetyltransferase in epigenetic signaling and disease. *J. Cell Physiol* **2014**, *229*, 1571−1574.

(8) Ullah, M.; Pelletier, N.; Xiao, L.; Zhao, S. P.; Wang, K.; Degerny, C.; Tahmasebi, S.; Cayrou, C.; Doyon, Y.; Goh, S. L.; Champagne, N.; Cote, J.; Yang, X. J. Molecular architecture of quartet MOZ/MORF histone acetyltransferase complexes. *Mol. Cell. Biol.* **2008**, *28*, 6828−6843.

(9) Laue, K.; Daujat, S.; Crump, J. G.; Plaster, N.; Roehl, H. H.; Kimmel, C. B.; Schneider, R.; Hammerschmidt, M. The multidomain protein Brpf1 binds histones and is required for Hox gene expression and segmental identity. *Development* **2008**, *135*, 1935−1946.

(10) Mishima, Y.; Miyagi, S.; Saraya, A.; Negishi, M.; Endoh, M.; Endo, T. A.; Toyoda, T.; Shinga, J.; Katsumoto, T.; Chiba, T.; Yamaguchi, N.; Kitabayashi, I.; Koseki, H.; Iwama, A. The Hbo1-Brd1/Brpf2 complex is responsible for global acetylation of H3K14 and required for fetal liver erythropoiesis. *Blood* **2011**, *118*, 2443−2453.
(11) Nyegaard, M.; Severinsen, J. E.; Als, T. D.; Hedemand, A.; Straarup, S.; Nordentoft, M.; McQuillin, A.; Bass, N.; Lawrence, J.; Thirumalai, S.; Pereira, A. C.; Kandaswamy, R.; Lydall, G. J.; Sklar, P.; Scolnick, E.; Purcell, S.; Curtis, D.; Gurling, H. M.; Mortensen, P. B.; Mors, O.; Borglum, A. D. Support of association between BRD1 and both schizophrenia and bipolar affective disorder. *Am. J. Med. Genet., Part B* **2010**, *153B*, 582−591.
(12) Qin, S.; Jin, L.; Zhang, J.; Liu, L.; Ji, P.; Wu, M.; Wu, J.; Shi, Y. Recognition of unmodified histone H3 by the first PHD finger of bromodomain-PHD finger protein 2 provides insights into the regulation of histone acetyltransferases monocytic leukemic zinc-finger protein (MOZ) and MOZ-related factor (MORF). *J. Biol. Chem.* **2011**, *286*, 36944−36955.
(13) Vezzoli, A.; Bonadies, N.; Allen, M. D.; Freund, S. M.; Santiveri, C. M.; Kvinlaug, B. T.; Huntly, B. J.; Gottgens, B.; Bycroft, M. Molecular basis of histone H3K36me3 recognition by the PWWP domain of Brpf1. *Nat. Struct. Mol. Biol.* **2010**, *17*, 617−619.
(14) Poplawski, A.; Hu, K.; Lee, W.; Natesan, S.; Peng, D.; Carlson, S.; Shi, X.; Balaz, S.; Markley, J. L.; Glass, K. C. Molecular insights into the recognition of N-terminal histone modifications by the BRPF1 bromodomain. *J. Mol. Biol.* **2014**, *426*, 1661−1676.
(15) Lalonde, M. E.; Avvakumov, N.; Glass, K. C.; Joncas, F. H.; Saksouk, N.; Holliday, M.; Paquet, E.; Yan, K.; Tong, Q.; Klein, B. J.; Tan, S.; Yang, X. J.; Kutateladze, T. G.; Cote, J. Exchange of associated factors directs a switch in HBO1 acetyltransferase histone tail specificity. *Genes Dev.* **2013**, *27*, 2009−2024.
(16) Hewings, D. S.; Rooney, T. P.; Jennings, L. E.; Hay, D. A.; Schofield, C. J.; Brennan, P. E.; Knapp, S.; Conway, S. J. Progress in the development and application of small molecule inhibitors of bromodomain-acetyl-lysine interactions. *J. Med. Chem.* **2012**, *55*, 9393−9413.
(17) Garnier, J. M.; Sharp, P. P.; Burns, C. J. BET bromodomain inhibitors: a patent review. *Expert. Opin. Ther. Pat.* **2014**, *24*, 185−199.
(18) Chung, C.; Dean, A. W.; Woolven, J. M.; Bamborough, P. Fragment-based discovery of bromodomain inhibitors part 1: inhibitor binding modes and implications for lead discovery. *J. Med. Chem.* **2012**, *55*, 576−586.
(19) Bamborough, P.; Diallo, H.; Goodacre, J. D.; Gordon, L.; Lewis, A.; Seal, J. T.; Wilson, D. M.; Woodrow, M. D.; Chung, C. W. Fragment-based discovery of bromodomain inhibitors part 2: optimization of phenylisoxazole sulfonamides. *J. Med. Chem.* **2012**, *55*, 587−596.
(20) Hewings, D. S.; Fedorov, O.; Filippakopoulos, P.; Martin, S.; Picaud, S.; Tumber, A.; Wells, C.; Olcina, M. M.; Freeman, K.; Gill, A.; Ritchie, A. J.; Sheppard, D. W.; Russell, A. J.; Hammond, E. M.; Knapp, S.; Brennan, P. E.; Conway, S. J. Optimization of 3,5-dimethylisoxazole derivatives as potent bromodomain ligands. *J. Med. Chem.* **2013**, *56*, 3217−3227.
(21) Zhao, L.; Cao, D.; Chen, T.; Wang, Y.; Miao, Z.; Xu, Y.; Chen, W.; Wang, X.; Li, Y.; Du, Z.; Xiong, B.; Li, J.; Xu, C.; Zhang, N.; He, J.; Shen, J. Fragment-based drug discovery of 2-thiazolidinones as inhibitors of the histone reader BRD4 bromodomain. *J. Med. Chem.* **2013**, *56*, 3833−3851.
(22) Filippakopoulos, P.; Picaud, S.; Mangos, M.; Keates, T.; Lambert, J. P.; Barsyte-Lovejoy, D.; Felletar, I.; Volkmer, R.; Muller, S.; Pawson, T.; Gingras, A. C.; Arrowsmith, C. H.; Knapp, S. Histone recognition and large-scale structural analysis of the human bromodomain family. *Cell* **2012**, *149*, 214−231.
(23) Tapia, I.; Alonso-Cires, L.; Lopez-Tudanca, P. L.; Mosquera, R.; Labeaga, L.; Innerarity, A.; Orjales, A. 2,3-Dihydro-2-oxo-1H-benzimidazole-1-carboxamides with selective affinity for the 5-HT(4) receptor: synthesis and structure-affinity and structure-activity relationships of a new series of partial agonist and antagonist derivatives. *J. Med. Chem.* **1999**, *42*, 2870−2880.
(24) Deplus, R.; Delatte, B.; Schwinn, M. K.; Defrance, M.; Mendez, J.; Murphy, N.; Dawson, M. A.; Volkmar, M.; Putmans, P.; Calonne, E.; Shih, A. H.; Levine, R. L.; Bernard, O.; Mercher, T.; Solary, E.; Urh, M.; Daniels, D. L.; Fuks, F. TET2 and TET3 regulate GlcNAcylation and H3K4 methylation through OGT and SET1/COMPASS. *EMBO J.* **2013**, *32*, 645−655.